ACS Sustainable Chemistry & Engineering

Research Article

pubs.acs.org/journal/ascecg

Design of Magnetic Attapulgite/Fly Ash/Poly(acrylic acid) Ternary Nanocomposite Hydrogels and Performance Evaluation as Selective Adsorbent for Pb^{2+} Ion

Liping Jiang[†,‡] and Peng Liu*[,†]

[†]State Key Laboratory of Applied Organic Chemistry and Institute of Polymer Science and Engineering, College of Chemistry and Chemical Engineering, Lanzhou University, Lanzhou 730000, China

[‡]Department of Chemistry, Gansu Lianhe University, Lanzhou 730000, China

ABSTRACT: A facile inverse suspension polymerization approach was developed for the preparation of the magnetic attapulgite/fly ash/poly(acrylic acid) (ATP/FA/PAA) ternary nanocomposite hydrogels, after the inorganic materials were *in situ* modified. In the optimized preparation condition obtained via the $L_9(3^4)$ orthogonal experiments, about 95% of the monomer had been grafted onto the inorganic materials to form the three-dimensional cross-linking network of the ternary nanocomposite hydrogels. The ternary nanocomposite hydrogels exhibited good adsorption selectivity toward the Pb^{2+} ion, and the adsorbed ion could be completely desorbed with HCl aqueous solution. Furthermore, the ternary nanocomposite hydrogels possessed high mechanical stability and magnetic property. These features as well as their low cost make them a potential adsorbent for treating Pb^{2+}-contaminated water.

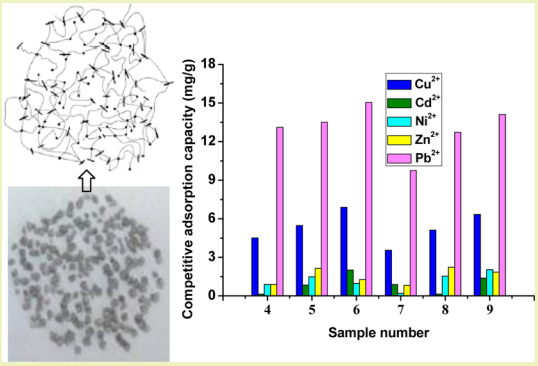

KEYWORDS: *Ternary nanocomposite hydrogels, Inverse suspension polymerization, Three-dimensional network, Selective adsorbent, Heavy metal*

INTRODUCTION

Heavy metals are considered to be one of the main global pollutants in the environment because they can accumulate in living tissues throughout the food chain due to their nonbiodegradability and thus have potentially detrimental effects on all living species. Therefore, removal of toxic heavy metals from contaminated water is of great importance. In comparison with the other processes (such as coagulation/precipitation and coprecipitation/adsorption) for the treatment of the polluted aqueous effluents, the sorption process possesses some distinct advantages, such as flexibility in design and operation, producing superior effluent suitable for reuse without other pollutants.[1] Furthermore, certain types of contaminants could be removed with a proper adsorbent. For the recovery and removal of heavy metal ions, polymeric adsorbents are more effective due to their structure, cost effectiveness, availability of different sorbents, easy handling, reusability, and chemical and mechanical strength.[2]

Recently, hydrogels with a three-dimensional (3-D) network as well as functional groups are well documented to be used for the removal of heavy metals from aqueous solutions because of their plentiful ionic functional groups.[3−5] Hydrogels can swell considerably in aqueous media without dissolution, which is helpful for adsorbing and trapping metal ions. The unique swelling property of hydrogels and the porous structure make heavy metal ions more easily accessible to the functional groups in hydrogels. Nanomaterials have been incorporated into the hydrogels in the form of nanocomposite hydrogels in order to improve their mechanical strength[6,7] or provide a magnetic property.[8,9] In most of the nanocomposite hydrogels reported, the nanomaterials were only mixed into the nanocomposites that were cross-linked with the organic cross-linkers such as *N,N′*-methylenebis(acrylamide) (MBA)[6,7] or glutaraldehyde.[8,9] In our previous work, the functional attapulgite nanorods (org-ATP) have been used as both the cross-linker and the strengthening agent in facile inverse suspension polymerization. Thus, the attapulgite/poly(acrylic acid) (ATP/PAA) nanocomposite hydrogels with the well-defined 3-D network were obtained without any foreign organic cross-linker added.[10]

Fly ash (FA) is a waste from thermal power plants, steel mills, etc. It is found in abundance in the world and has been utilized as a low-cost adsorbent.[11] In the present work, the magnetic FA particles were separated and functionalized as cross-linkers instead of the traditional cross-linker for the preparation of novel magnetic attapulgite/fly ash/poly(acrylic cid) (ATP/FA/PAA) ternary nanocomposite hydrogels, as well as the ATP nanorods. In the inverse suspension polymerization process, acrylic acid (AA) is grafted onto the inorganic skeleton

Received: January 15, 2014
Revised: May 12, 2014
Published: May 21, 2014

established by the functionalized ATP and FA to form the ternary nanocomposite hydrogels with the 3-D network. The inorganic materials not only lower the cost of the production significantly but also improve the mechanical strength, thermal stability, chemical resistance, and dimensional stability of the products. Furthermore, the introduction of the magnetic FA particles could provide the magnetic separation function to the ternary nanocomposite hydrogels. The preparation of the ternary nanocomposite hydrogels was optimized with a series of $L_9(3^4)$ orthogonal experiments.[12] Finally, the ternary nanocomposite hydrogels were used as the selective adsorbent for Pb^{2+} ion.

EXPERIMENTAL METHODS

Materials. The attapulgite mineral was obtained from the R&D Center of Xuyi Attapulgite Applied Technology, Lanzhou Institute of Chemical Physics, Chinese Academy of Sciences. It was first baked at 180 °C to remove organic compounds and then grinded in distilled water and acidified in 4.0 mol/L HCl aqueous solution for 6 h to release more surface hydroxyl groups.[13] The ATP dispersion was filtrated, and a filter cake of ATP was obtained with solid content about 20%.

FA (main constituents: SiO_2, 58.64%; Al_2O_3, 21.32%; CaO, 5.02%; Fe_2O_3, 7.20%; MgO, 1.58%; and MnO, 2.23%) with a diameter of 0.5−10 μm was obtained from Datang Gansu Power Generation Co., Ltd., Lanzhou, China. The FA powder was treated with 0.10 mol/L HCl aqueous solution for 6 h to release its surface hydroxyl groups[14] and then washed and dried at 120 °C for 2 h. The activated fly ash was further grinded in a mortar and filtrated with an 800-mesh screen, followed by magnetic selection to obtain the activated magnetic fly ash for use.

AA (analytical reagent grade) was obtained from Tianjin Kaixin Chemical Industry Co., Ltd., Tianjin, China. Span-80 (analytical reagent grade) and liquid paraffin (chemical pure) were provided by Tianjin Guangfu Fine Chemical Research Institute, Tianjin, China. γ-Methacryloxypropyl trimethoxysilane (KH-570, industrial grade) was provided by Jiangsu Chenguang Silane Co., Ltd., Nanjing, China. All other reagents were used as received without any further purification. Double-distilled water was used throughout.

Preparation of ATP/FA/PAA Ternary Nanocomposite Hydrogels. The activated magnetic FA powders were dispersed into distilled water and then mixed with the ATP filter cake at a solid mass ratio of 1:1. The obtained mixture was dispersed in liquid paraffin with Span-80 as dispersant and ultrasonically oscillated for 1 h. KH-570 was added to the mixture at one-third of the total sum of ATP/FA and then stirred at room temperature for 0.5 h and ultrasonically dispersed for 2 h, followed by stirring at 40 °C for 6 h to obtain the KH-570 modified ATP/FA.

AA was predispersed in liquid paraffin with Span-80 as dispersant for about 1 h. This predispersion was added into the obtained dispersion of the KH-570-modified ATP/FA and stirred at room temperature for 0.5 h. After APS was added and stirred for 0.5 h, the mixture was stirred at 60 °C for 2 h, followed by 80 °C for 3 h under N_2 atmosphere to get the magnetic ATP/FA/PAA ternary nanocomposite hydrogel beads. The beads were washed with ether and distilled water in sequence, immersed in ammonia−water of pH in the range of 8−9 for 24 h, and extracted in distilled water for 48 h to remove the possible ungrafted poly(acrylic acid) (PAA). They were finally rinsed with ethanol and dried at 70 °C in a vacuum oven.

In the inverse suspension polymerization, the mass ratio of ATP/FA to AA (inorganic/AA), mass percentage of Span-80 in the total mass of water phase (Span-80%), mass percentage of APS in the total mass of AA (APS%), and oil−water mass ratio were optimized with a series of $L_9(3^4)$ orthogonal experiments (Table 1).

Adsorption Performance. A solution of mixed heavy metal ions was prepared by adding 0.1058 g of $CuCl_2$, 0.0896 g of $CdCl_2{\cdot}H_2O$, 0.2025 g of $NiCl_2{\cdot}6H_2O$, 0.1043 g of $ZnCl_2$, and 0.0799 g of $Pb(NO_3)_2$ in 500 mL aqueous HCl solution of pH 5.0. The concentration of each ion in this solution is expressed as C_0 (mg/L). Accurately weighed ternary nanocomposite hydrogel samples from 4 to 9 (0.1 g) (expressed as W (g)) were added into to 50 mL of the above solution and were stirred for 6 h. Then, the remaining concentrations of the five heavy metal ions were measured by an atomic absorption spectrometry (AA 240 atomic absorption spectrometer (AAS, Varian, U.S.A.)) and expressed as C_t (mg/L). All the values presented were averages of at least three measurements with the relative deviations of <5%. The competitive adsorption capacities (A, mg/g) of the samples from 4 to 9 were calculated with the following formula

$$A = (C_0 - C_t)/(20W) \quad (1)$$

Accurately weighed ternary nanocomposite hydrogel sample 6 (0.1 g) was added into the 50 mL of the 100 mg/L Pb^{2+} solution prepared with aqueous HCl solution at different pH values (1.0, 2.0, 3.0, 4.0, 5.0, or 6.0) and stirred for 6 h. The remaining Pb^{2+} concentrations were measured with AAS to calculate the adsorption capacity for Pb^{2+} at different pH values, with formula 1. After that, the adsorption time was investigated by stirring the accurately weighed ternary nanocomposite hydrogel sample 6 (0.1 g) in 50 mL of 100 mg/L Pb^{2+} solution at pH 5.0 for 1, 2, 3, 4, 5, 7, 9, 24, 36, or 48 h.

Adsorption Kinetics. The batch kinetic studies were carried out by stirring accurately weighed ternary nanocomposite hydrogel sample 6 (0.1 g) in a 50 mL solution of 100 mg/L Pb^{2+} ion at pH 5.0. After stirring for 48 h, the remaining Pb^{2+} concentration in the solution was determined. The obtained experimental data were analyzed with the pseudo-first order, pseudo-second order, and intraparticle diffusion models as follows[15]

The pseudo-first-order equation was represented by

$$1/q_t = k_1/(q_e \times t) + 1/q_e \quad (2)$$

where k_1 (h^{-1}) is the pseudo-first-order adsorption rate constant, q_t is the amount adsorbed at time t (h), and q_e denotes the amount adsorbed at equilibrium, both in mmol/g.

The pseudo-second-order equation can be expressed as

$$t/q_t = 1/(k_2 \times q_e^{\,2}) + t/q_e \quad (3)$$

where k_2 (g/(mmol/h)) is the adsorption rate constant of pseudo-second-order.

The linear form of the intraparticle diffusion equation is given by

$$\ln q_t = \ln k_i + 1/2 \ln t \quad (4)$$

where k_i (mmol/(g $h^{1/2}$)) is the intraparticle diffusion rate constant.

Adsorption Thermodynamic Analysis. The adsorption thermodynamic studies were carried out by stirring accurately weighed ternary nanocomposite hydrogel sample 6 (0.1 g) in a 50 mL Pb^{2+} aqueous solution at pH 5.0 with different concentrations (20, 40, 60, 80 and or mg/L). After stirring at 293, 303, and 313 K for 24 h, the remaining Pb^{2+} concentrations (C_e) in the solutions were determined with FAAS

Table 1. $L_9(3^4)$ Orthogonal Experiments on Preparation of Magnetic ATP/FA/PAA Ternary Nanocomposite Hydrogel Beads

	variables			
serial number	inorganic cross-linkers[a]: AA	Span-80%	APS%	oil−water mass ratio
1	1:1	1	0.5	2:1
2	1:1	3	1.0	3:1
3	1:1	5	1.5	4:1
4	1:3	1	1.0	4:1
5	1:3	3	1.5	2:1
6	1:3	5	0.5	3:1
7	1:5	1	1.5	3:1
8	1:5	3	0.5	4:1
9	1:5	5	1.0	2:1

[a]The mixture of FA and ATP at mass ratio of 1:1.

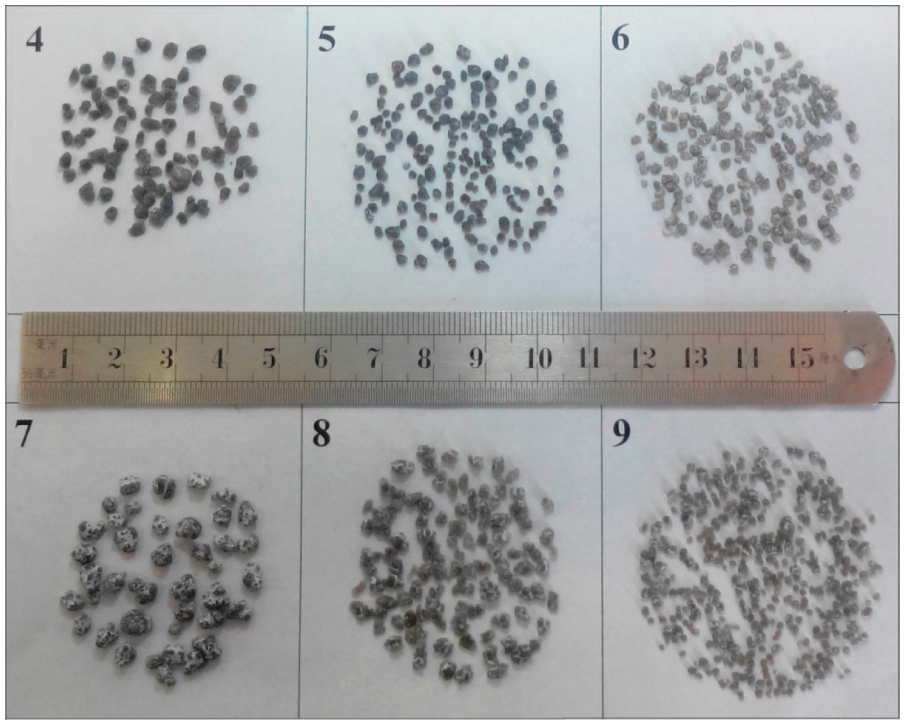

Figure 1. Appearance of ternary nanocomposite hydrogel bead samples 4−9.

to calculate the equilibrium adsorption capacity (q_e). The obtained experimental data were analyzed with the Langmuir (eq 5) and Freundlich (eq 6) adsorption isotherms as follows[10]

$$C_e/q_e = 1/(k_L \times q_L) + C_e/q_L \quad (5)$$

$$\ln q_e = \ln k_F + 1/n_F \ln C_e \quad (6)$$

where q_e (mg/g) and C_e (mg/L) represent the amount of adsorbed Pb^{2+} per unit mass of ATP/FA/PAA ternary nanocomposite hydrogel sample 6 and the concentration of the remaining Pb^{2+} in solution at equilibrium, respectively; q_L is the maximum monolayer adsorption capacity at a given temperature; k_L represents the equilibrium constant for the adsorption; k_F and n_F are system specific constants, k_F gives an indication for adsorption capacity (higher the k_F, higher the maximum capacity); $1/n_F$ is a measure of intensity of adsorption (value of n_F >1 represents favorable adsorption condition).

Desorption. After accurately weighed ternary nanocomposite hydrogel sample 6 (0.1 g) was stirred in a 50 mL solution of 100 mg/L of Pb^{2+} ion at pH 5.0 for 24 h, the ternary nanocomposite hydrogel sample 6 saturated with Pb^{2+} ion was filtrated, washed, wiped off the residual water on the surface, and then stirred in 50 mL of HCl aqueous solution with different concentrations (0.05, 0.10, 0.20, 0.30, 0.40, 0.60, or 0.80 mol/L) for 3 h. The concentration of the eluted Pb^{2+} (C_d) in each HCl aqueous solution was also measured by FAAS. The desorption ratios (R_d) of ATP/FA/PAA ternary nanocomposite hydrogel sample 6 with HCl aqueous solutions were calculated by the following formula

$$R_d = C_d/(C_0 - C_t) \times 100\% \quad (7)$$

Then, the desorption time was investigated by stirring ternary nanocomposite hydrogel sample 6 (0.1 g) saturated with Pb^{2+} in a 0.10 mol/L HCl aqueous solution for 0.5, 1.0, 1.5, 2.0, 2.5, or 3.0 h. Each R_d of sample 6 with a different desorption time was calculated with formula 5.

Analysis and Characterization. FT-IR spectra of the ATP, FA, KH-570-modified ATP/FA, ATP/FA/PAA ternary nanocomposite hydrogel sample 6, and Pb^{2+}-adsorbed ATP/FA/PAA ternary nanocomposite hydrogel sample 6 were characterized with an Avatar 360 FT-IR instrument (Nicolet, U.S.A.) in the range of 400−4000 cm^{-1} with a resolution of 4 cm^{-1} by the KBr pellet method.

The thoroughly dried ATP/FA/PAA ternary nanocomposite hydrogel beads were grinded into powder with mortar and characterized by TGA (TGA 2050 (TA Instruments, U.S.A.)) in order to evaluate the amount of the organic constituents grafted in the ternary nanocomposite hydrogels, in the range of 30−800 °C with a heating rate of 10 °C/min in N_2 atmosphere.

After being immersed in distilled water for 24 h to swell thoroughly, the swollen magnetic ATP/FA/PAA ternary nanocomposite hydrogel sample 6 was then dried in a freeze-dryer. The freeze-dried sample was then cut in half. The section of sample was observed by SEM (JSM-6380, JEOL, Ltd., Japan) to study its micromorphologies.

The magnetic ATP/FA/PAA ternary nanocomposite hydrogel sample 6 was thoroughly dried, grinded into powder, and measured with a vibrating sample magnetometer (VSM, Lakeshore 7400, U.S.A.) at room temperature to evaluate the specific saturation magnetization and coercive force.

The thoroughly dried and fully hydrated samples (being immersed into distilled water for 24 h) were subsequently weighed to calculate the water absorption ratio of the magnetic ATP/FA/PAA ternary nanocomposite hydrogels.

The magnetic ATP/FA/PAA ternary nanocomposite hydrogel beads were fully hydrated in distilled water and stirred in a high-speed agitator at 5000 rpm for 2 h. The damage rate of the beads was used to evaluate its anti-shearing ability. Likewise, four fully hydrated microgel beads were put under a glass board with a 3 kg load on it, and the damage rate was used to estimate the pressure resistance of the magnetic ATP/FA/PAA ternary nanocomposite hydrogel beads.

RESULTS AND DISCUSSION

Effects of Polymerization Conditions on Formation of Magnetic ATP/FA/PAA Ternary Nanocomposite Hydrogel Beads. The effects of the polymerization conditions, such as the mass ratio of ATP/FA to AA (Inorganic/AA), mass percentage of Span-80 in the total mass of water phase (Span-80%), mass percentage of APS in the total mass of AA (APS%), and oil−water mass ratio in the inverse suspension polymer-

dx.doi.org/10.1021/sc500031z | ACS Sustainable Chem. Eng. 2014, 2, 1785−1794

ization, were investigated with a series of $L_9(3^4)$ orthogonal experiments (Table 1). Specimens 1−3 appeared to be viscous fluid, while specimens 4−9 produced the magnetic ATP/FA/PAA ternary nanocomposite hydrogel beads, indicating that the amount of AA had an obvious effect on the formation of the ternary nanocomposite hydrogel beads. The inverse suspension polymerization is a heterogeneous liquid−liquid dispersion in which the size of the aqueous droplets (dispersed phases) changes during the whole polymerization procedure and is determined by the balance between the rates of breakup and coalescence of the droplet.[16] With the increase in the concentration of AA, the formation rate of PAA at the beginning of the polymerization increases and the viscosity of the aqueous droplets increases. The process consequently slows the rate of breakup of the droplets and promotes the balance between the droplet breakup and coalescence. As a result, it becomes easier to form the magnetic ATP/FA/PAA ternary nanocomposite hydrogel beads with the increase in the dosage of AA in the specimens.

In addition, the diameters of ternary nanocomposite hydrogel bead samples 6 and 9 are slightly smaller and more uniform than the other samples (Figure 1), implying that the Span-80 concentration has a certain effect on the size of the beads, as reported previously.[17,18] Span-80 is used as dispersant in this water-in-oil dispersion to enhance the stability of the droplets and prevent them from coalescence. The surface tension of the droplets decreases with the increase in the Span-80 concentration, which promotes the breakup of droplets and leads to a small size of particle. However, the viscosity of the droplets becomes higher with the polymerization of AA. Because the speed of droplet breakup is mainly determined by the resisting viscous forces instead of the interfacial tension forces, the size of the droplets reaches a more fixed value when the balance between the breakup and coalescence is established. On the other hand, the lower interfacial tension due to the use of Span-80 increases the stability of the droplets, which results in a shorter transition stage and a more stable dispersion during the inverse suspension polymerization, leading to an almost constant size of the droplets. Therefore, the average size of the final beads decreases and becomes narrower with an increased dosage of Span-80.

The magnetic ATP/FA/PAA ternary nanocomposite hydrogel beads showed the diameter of 1−5 mm and precipitated immediately once the stirring was stopped, indicating that the beads could be easily separated from the polymerization mixture. During the purification by immersing the beads in ammonia−water of pH 8−9 for 24 h and extracting in distilled water for 48 h, the ATP/FA/PAA ternary nanocomposite hydrogel beads were insoluble and maintained their spherical appearance. This implies that AA has polymerized and grafted onto the inorganic skeleton of FA and ATP to form a 3-D network without any organic cross-linker (as shown in Figure 2). Furthermore, the surfaces of the ATP/FA/PAA ternary nanocomposite hydrogel beads were nonsticky after being rinsed with ethanol and baked at 70 °C in a vacuum oven, as shown in Figure 1, indicating a good stability.

Aqueous Swelling. The thoroughly dried and fully hydrated ATP/FA/PAA ternary nanocomposite hydrogel beads were accurately weighted. The mass ratio of the absorbed water to the dry sample was calculated to estimate the water absorption ratio (Figure 3). The trend of the water absorption ratio is obviously divided into two groups: from 4 to 6 (Group 1) and from 7 to 9 (Group 2). Combined with the data in Table 1, one can find that the dosage of Span-80 increases with the maintained dosage of AA in each group. It indicates that the concentration of Span-80 has a certain effect on the water absorption ratio of the ATP/FA/PAA ternary nanocomposite hydrogel beads. In each group, the particle size decreased (Figure 1) and the water absorption ratio increased (Figure 3) with increasing the Span-80 concentration.

Figure 2. Structural model of the 3-D network with both magnetic particles (dots) and ATP nanorods (lines) as cross-linkers.

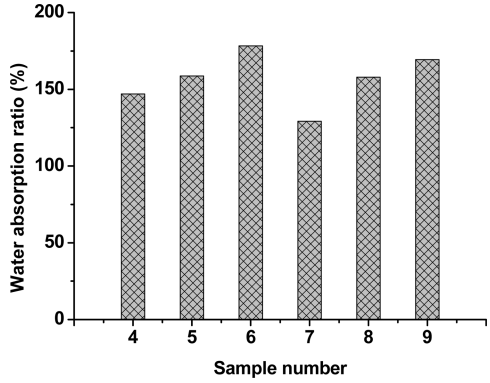

Figure 3. Water absorption ratios of the FA/PAA/ATP nanocomposite magnetic beads.

In addition, the water absorption ratios of the samples in Group 1 were higher than those of the samples in Group 2 with the same Span-80 concentration, implying that the grid in the 3-D network of the ATP/FA/PAA ternary nanocomposite hydrogel beads becomes smaller when the AA dosage increases from 75% to 83% (the mass percentage of AA in the total mass of FA, ATP, and AA). This has a negative effect on the aqueous swelling of the products.[19]

Adsorption Selectivity. The competitive adsorption performance of the ATP/FA/PAA ternary nanocomposite hydrogel beads toward five heavy metal ions (Cu^{2+}, Cd^{2+}, Ni^{2+}, Zn^{2+}, and Pb^{2+}) was used to investigate their adsorption selectivity. It was found that all the carboxyl group containing ATP/FA/PAA ternary nanocomposite hydrogel beads exhibited good adsorption selectivity to Pb^{2+} ion (Figure 4) due to the difference in the metal ion properties such as ionic radius, electronegativity, and ionization potential.[20,21] Furthermore, the competitive adsorption capacity to Pb^{2+} from sample 4 to 9 changed the same way as the water absorption ratio did. It means that the competitive adsorption capacity increased with the decrease in the sizes of the ATP/FA/PAA ternary nanocomposite hydrogel beads.

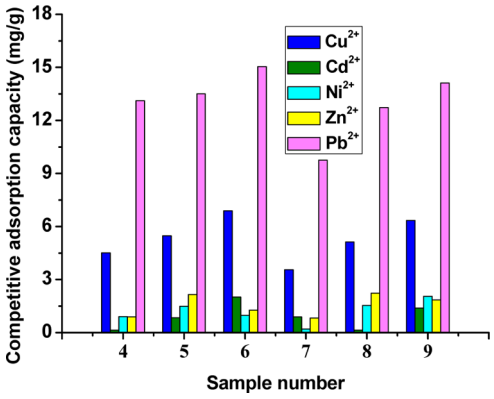

Figure 4. Adsorption selectivity of the FA/PAA/ATP nanocomposite magnetic beads to Ni^{2+}, Cu^{2+}, Cd^{2+}, Zn^{2+}, and Pb^{2+} ions.

In addition, compared with samples 4−6 (Group 1), samples 7−9 (Group 2), with the higher cross-linking density and smaller cross-linking grid as above-described, were unfavorable for the adsorption of Pb^{2+}. Considering all above factors comprehensively, ATP/FA/PAA ternary nanocomposite hydrogel bead sample 6 should be the optimal selective adsorbent to Pb^{2+} ion.

Characterization of ATP/FA/PAA Ternary Nanocomposite Hydrogel Bead Sample 6. The preparations of the activated FA, activated ATP, KH-570-modified ATP/FA, and ATP/FA/PAA ternary nanocomposite hydrogel bead (sample 6) were verified by FT-IR (Figure 5). Compared with the FT-

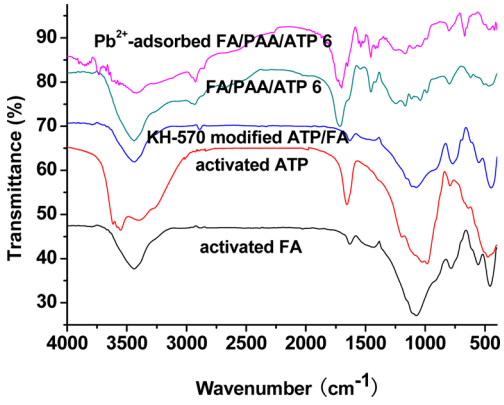

Figure 5. FT-IR spectra of the activated FA, activated ATP, KH-570-modified ATP/FA, and ATP/FA/PAA ternary nanocomposite hydrogel bead (sample 6).

IR spectra of activated FA and ATP, a very weak absorbance peak in the range of 2850−2940 cm^{-1} representing the C−H stretching band appeared in the spectrum of the KH-570-modified ATP/FA, which proves that KH-570 has been modified onto the inorganic materials. After the inverse suspension polymerization, the C−H stretching band became stronger, and two new characteristic absorbance peaks at 1714 and 1450 cm^{-1}, corresponding to the C═O stretch band of the carboxyl group and the stretch of C−O and the deformation vibration of OH appeared,[22] indicating that AA has been successfully grafted on the inorganic skeleton of the FA and ATP to form the ATP/FA/PAA ternary nanocomposite hydrogels with the 3-D cross-linking network through the bridge of KH-570.

The TGA result of ATP/FA/PAA ternary nanocomposite hydrogel bead sample 6 (Figure 6) showed that the organic

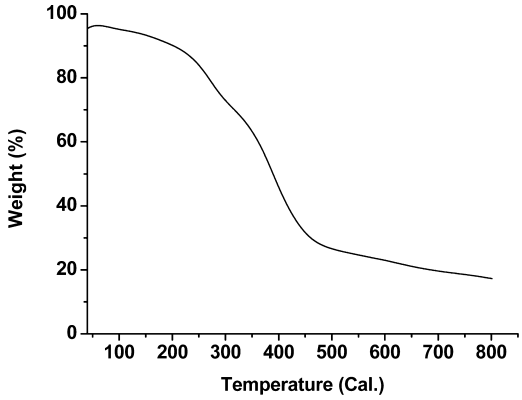

Figure 6. TGA curve of ATP/FA/PAA ternary nanocomposite hydrogel bead (sample 6).

composition in ATP/FA/PAA ternary nanocomposite hydrogel bead sample 6 was about 71%. Compared to its theoretical value of 75%, the utilization ratio of AA in sample 6 could be calculated to be 94.7%. This means that almost all the monomer AA had been grafted onto the inorganic materials to form the 3-D cross-linking network. It is very promising as a candidate of industry applications.

The specific saturation magnetization and coercivity of the thoroughly dried sample 6 were measured with a vibrating sample magnetometer at room temperature in the range from −11,000 to 11,000 Oe. As shown in Figure 7, the specific

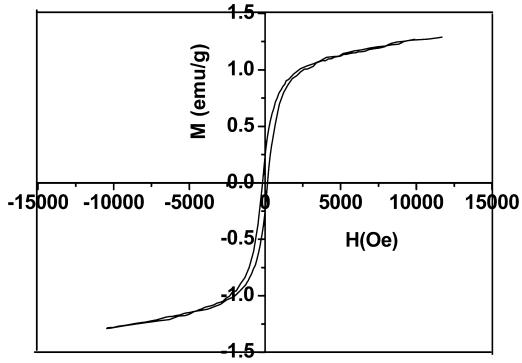

Figure 7. Magnetization curve of ATP/FA/PAA ternary nanocomposite hydrogel bead (sample 6).

saturation magnetization of Sample 6 was 1.3 emu/g, and its coercivity was about 140 Oe, indicating that the obtained ATP/FA/PAA ternary nanocomposite hydrogel sample 6 had a certain magnetic induction and is easy to demagnetize. This magnetic feature of ATP/FA/PAA ternary nanocomposite hydrogel sample 6 provides a convenient approach for separation by applying external magnetic fields.[23]

The SEM micrograph of the fracture surface of Freeze-dried sample 6 is presented in Figure 8. It is shown that ATP/FA/PAA ternary nanocomposite hydrogel sample 6 is porous (at the micrometer level) and formed by the connection of the micrometer-scaled clusters of the inorganic materials. The antipressure resistance and the anti-shearing ability of sample 6 were evaluated. The beads of sample 6 were not broken after the antipressure test as shown Figure 9 and appeared only

dx.doi.org/10.1021/sc500031z | ACS Sustainable Chem. Eng. 2014, 2, 1785−1794

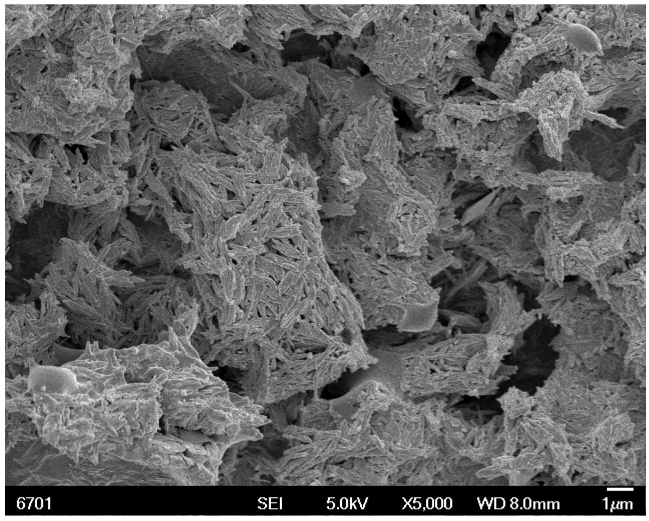

Figure 8. SEM image of the fracture surface of ATP/FA/PAA ternary nanocomposite hydrogel (sample 6).

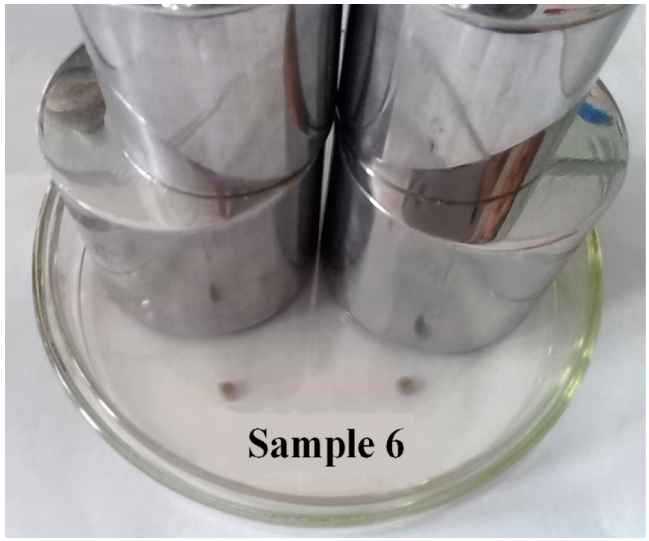

Figure 9. Photo of four beads of sample 6 under a 3 kg load.

slightly fluffy on their surface after stirring for 2 h at 5000 rpm as shown in Figure 10. The results suggest that sample 6 has a long service lifetime due to its excellent mechanical stability and thus further reducing the overall cost.

Adsorption Property of Sample 6 Toward Pb^{2+} Ion. Figure 11 shows the media pH dependence of the adsorption

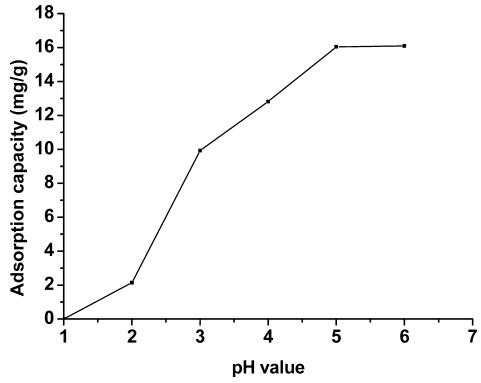

Figure 11. pH dependence of the adsorption capacity of ATP/FA/PAA ternary nanocomposite hydrogel sample 6 to the Pb^{2+} ion.

capacity of ATP/FA/PAA ternary nanocomposite hydrogel sample 6 to the Pb^{2+} ion. At pH lower than 2, the concentration of H^+ is high, which lowers the concentration of the free $-COO^-$ groups and consequently decreases the electrostatic attraction between $-COO^-$ and Pb^{2+}. By increasing the media pH value from 2 to 3, the H^+ concentration decreases and more free $-COO^-$ groups are produced, which favors the interaction between $-COO^-$ and Pb^{2+} and leads to a significant increase in the adsorption capacity of sample 6 to Pb^{2+}. The increase in the adsorption capacity slowed when pH was increased from 3 to 5 due to the buffer between $-COOH$ and $-COO^-$.[24] With the further increase in the media pH values, the equilibrium between $-COOH$ and $-COO^-$ is established due to the pK_a of PAA being about 4.7[25] and the adsorption capacity of sample 6 to Pb^{2+} approaching saturation, about 16 mg/g, as shown in Figure 11. Therefore, the optimum pH value for the adsorption of sample 6 to Pb^{2+} was selected to be 5 in order to increase the adsorption efficiency and avoid the hydrolysis of Pb^{2+} in the neutral medium.[26]

Figure 12 shows that the adsorption capacity of sample 6 to Pb^{2+} increases sharply in the first 9 h, implying that Pb^{2+} interacts rapidly with the $-COO^-$ groups on the surface of the ATP/FA/PAA beads. The concentration of Pb^{2+} on the surface is then higher than that inside, which produces the osmotic pressure and drives the permeation of Pb^{2+} into the beads. However, Pb^{2+} adsorbed on the surface hinders the migration of Pb^{2+} into the inner part of the ATP/FA/PAA beads due to

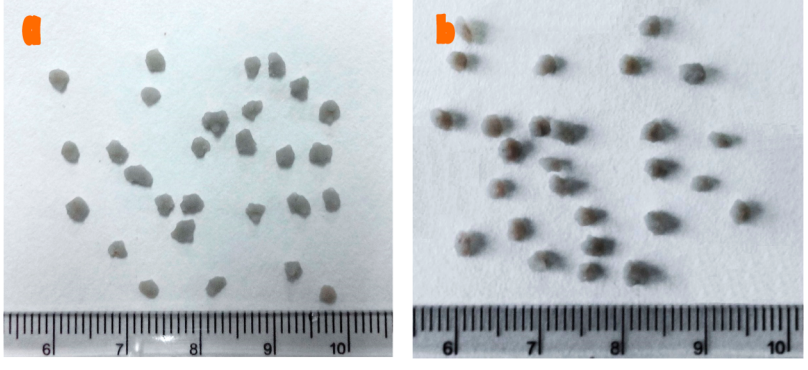

Figure 10. Photos of swollen sample 6 before (a) and after (b) the anti-shearing test by stirring at 5000 rpm for 2 h.

dx.doi.org/10.1021/sc500031z | ACS Sustainable Chem. Eng. 2014, 2, 1785−1794

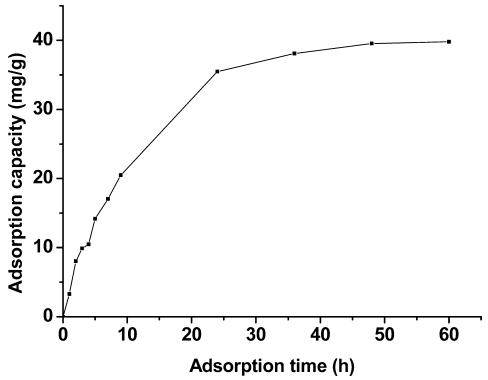

Figure 12. Time dependence of the adsorption capacity of ATP/FA/PAA ternary nanocomposite hydrogel sample 6 to Pb^{2+} ion.

the elastic shrinkage of PAA and the electrostatic repulsion between Pb^{2+} on the surface and Pb^{2+} in the solution.[10] Therefore, the adsorption capacity of sample 6 to Pb^{2+} increased gradually from 9 to 24 h when the migration of Pb^{2+} dominated over the impediment, and then, as presented in Figure 12, it reached saturation level around 38 mg/g when the equilibrium between these two conflicting factors was established after 24 h.

The characteristic absorbance peaks at 1714 and 1450 cm^{-1} of the carboxyl groups in the ATP/FA/PAA ternary nanocomposite hydrogel shifted to 1701 and 1456 cm^{-1} after adsorption of the Pb^{2+} ion (Figure 5). It revealed that the Pb^{2+} ion might be adsorbed via the chelating interaction with the carboxyl groups in the ATP/FA/PAA ternary nanocomposite hydrogel. Furthermore, in the 6 h of the competitive adsorption for the five heavy metal ions, the total adsorption capacity was 0.2350 mmol/g of ATP/FA/PAA ternary nanocomposite hydrogel sample 6. It was much higher than the equilibrium adsorption capacity of Pb^{2+} in 60 h of 0.1921 mmol/g. Thus, the five heavy metal ions might be adsorbed onto ATP/FA/PAA ternary nanocomposite hydrogel sample 6 via different interaction, and the adsorption selectivity for Pb^{2+} might be explained by the difference in the physical and chemical properties of these metal ions, such as ionic radius, electronegativity, and ionization potential.[20,21]

Calculated correlation coefficients, both linear and nonlinear, for pseudo-first-order and pseudo-second-order models by using a regression procedure are shown in Table 2. Because the calculated correlation coefficients are closer to unity for the pseudo-second-order kinetic model than the pseudo first-order kinetic model, the adsorption kinetics could well be approximated more favorably by the pseudo-second-order kinetic model.[15] Moreover, the calculated equilibrium adsorption capacity value, $q_{e,cal}$, was closer to the experimental $q_{e\ exp}$ value.

The intraparticle diffusion plots showed the multi-linearity correlation that indicated that two steps occurred during the adsorption process (Figure 13c). The first initial linear portion was followed by a plateau. The initial linear portion represented the intraparticle diffusion, while the plateau corresponds to equilibrium. The straight line did not pass the origin, indicating that the intraparticle diffusion is not the sole rate-limiting process.[27] The correlation coefficients (Table 2) showed a good fit for both portions, whereby the intraparticle diffusion rate constant, k_i ($t \leq 9$ h), represented the first linear portion, while k_i ($t > 9$ h) represented the equilibrium portion.

At the beginning of the experiment, the chemisorption on the outer surface of the beads seems to be the rate-limiting step.[28] However, after 9 h, the intraparticle diffusion seems to be rate-controlling step. During the adsorption process to Pb^{2+}, the adsorbed Pb^{2+} ions on the surface of the ATP/FA/PAA beads act as metallic ion cross-linkers and increase the number of cross-linking points,[29] which in turn increases the elastic shrinkage of polymer chains and therefore decreases the grid in the 3-D structure of the ATP/FA/PAA beads. As a result, the further permeation of Pb^{2+} ions is hindered. On the other hand, the electrostatic repulsion between Pb^{2+} on the surface of the beads and Pb^{2+} in the solution also has a negative impact on the further adsorption of Pb^{2+}.

The linear plots of C_e/q_e against C_e of the Langmuir isotherm and ln C_e against ln q_e of the Freundlich isotherm are shown in Figure 14. The maximum monolayer adsorption capacity q_L and the Freundlich constants n_F of the adsorption of the Pb^{2+} ion on ternary nanocomposite hydrogel sample 6 were calculated from the slopes of the plots. R_L^2 of the fitted lines with the linear Langmuir isotherm equation and R_F^2 of the fitted lines with the linear Freundlich isotherm equation were both higher than 0.95, indicating that the adsorption of Pb^{2+} on the ternary nanocomposite hydrogel can be evaluated by both the Langmuir and the Freundlich models. On the other hand, R_F^2 is closer to 1 than R_L^2 is, implying that the adsorption was not as homogeneous as assumed in the Langmuir model, namely, the Freundlich isotherm should be more suitable to evaluate the adsorption here. The results from the Langmuir isotherms revealed that the maximum monolayer adsorption capacities of Pb^{2+} on the surface of the ternary nanocomposite hydrogel were 91.8 mg/g at 293 K, 111.4 mg/g at 303 K, and

Table 2. Kinetic Parameters for Pb^{2+} Adsorption by ATP/FA/PAA Ternary Nanocomposite Hydrogel Sample 6

$q_{e,exp}$ (mmol/g)	0.1921			
Pseudo-first-order				
k_1 (h^{-1})	16.22			
$q_{e,cal}$ (mmol/g)	0.2867			
R^2	0.9816 (linear)			0.9868 (nonlinear)
Pseudo-second-order				
k_2 (g/(mmol h))	0.3367			
$q_{e,\ cal}$ (mmol/g)	0.2389			
R^2	0.9931 (linear)			0.9956 (nonlinear)
Intraparticle kinetic		**Linear**		**Nonlinear**
	$t \leq 9$		$t > 9$	
K_i (mmol/(g $h^{1/2}$))	0.0185		0.1141	
R^2	0.9632		0.9481	0.9899

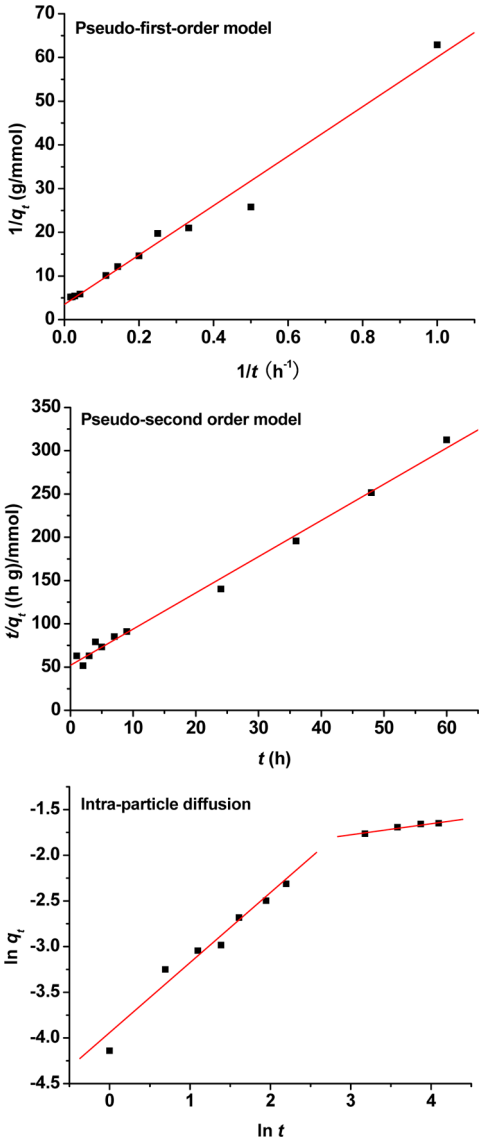

Figure 13. Pseudo-first order plot, pseudo-second order plot, and intraparticle diffusion kinetics for the adsorption of the Pb^{2+} ion on ternary nanocomposite hydrogel sample 6.

179.9 mg/g at 313 K, indicating that the saturated adsorption capacities increased with increasing temperature. In addition, the increase in the initial concentration of Pb^{2+} leads to the increase in osmotic pressure, and subsequently the increase in elastic stretch of the PAA chain segments, which expands the grid size of the ATP/FA/PAA microgels and drives the further adsorption of Pb^{2+} until the equilibrium between the osmotic pressure and the elastic shrinkage stress of the PAA chain segments. As a result, an increased equilibrium absorption capacity was also observed with increasing the initial concentrations of Pb^{2+} at a constant temperature in Figure 14. The Freundlich isotherms showed that n_F of the ATP/FA/PAA microgels toward Pb^{2+} were 1.2 at 293 K, 1.2 at 303 K, and 1.1 at 313 K. All the n_F values were higher than 1, indicating that favorable adsorption occurred under above conditions.[30]

Desorption of Pb^{2+} from Sample 6. H^+ in the solution restrains the transition of the −COOH groups into the $-COO^-$ groups and competes against the interaction between the $-COO^-$ groups and Pb^{2+}.[31] Besides, Cl^- reacts with the

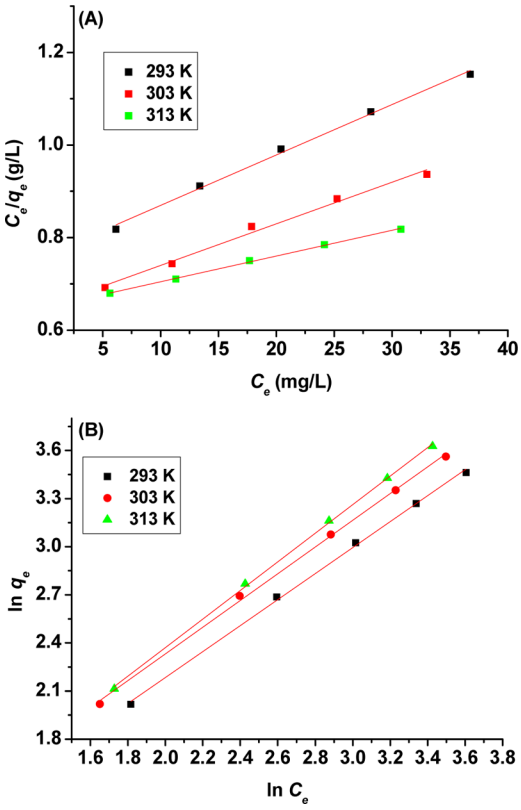

Figure 14. Linear plots of Langmuir (A) and Freundlich (B) isotherms for the adsorption of the Pb^{2+} ion on ternary nanocomposite hydrogel sample 6.

Pb^{2+} ions adsorbed in the ATP/FA/PAA beads to form certain complex anions such as $PbCl_3^-$ and $PbCl_4^{2-}$,[32] which drives Pb^{2+} to break away from the ATP/FA/PAA beads into the solution. Therefore, the HCl aqueous solution was selected as the eluant for the desorption of the Pb^{2+} from the ATP/FA/PAA beads (sample 6). It was found that the adsorbed Pb^{2+} was totally released from the ATP/FA/PAA beads into HCl aqueous solution with concentration of 0.1 or 0.2 mol/L (Figure 15).

However, the two reactions will reach equilibrium when the concentration of the HCl aqueous solutions is further increased. Pb^{2+} could precipitate (in the form of $PbCl_2$)[32] and accumulate on the surface of the ATP/FA/PAA beads, which hinders the further release of Pb^{2+}. As a result, the

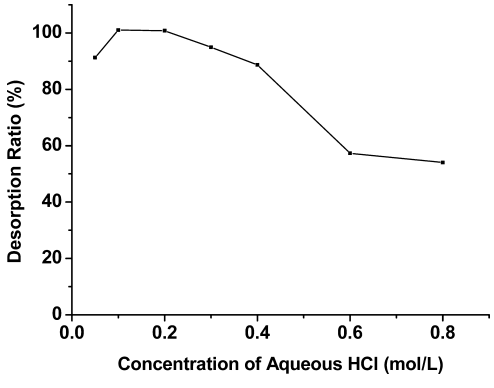

Figure 15. Desorption ratio of sample 6 saturated with Pb^{2+} with HCl solution for 3 h.

dx.doi.org/10.1021/sc500031z | ACS Sustainable Chem. Eng. 2014, 2, 1785−1794

desorption ratio of Pb^{2+} from sample 6 decreased when the concentration of the HCl aqueous solution was higher than 0.2 mol/L, as shown in Figure 15. So the optimum concentration of the HCl aqueous solutions for the desorption of Pb^{2+} from sample 6 was around 0.1 mol/L.

Then the equilibrium desorption time was investigated with 0.1 mol/L HCl aqueous solution as the eluant. In the first 0.5 h, Pb^{2+} was quickly eluted from the outer layer of the ATP/FA/PAA beads into the HCl aqueous solution, as shown in Figure 16. The elution then slowed, implying that the intraparticle

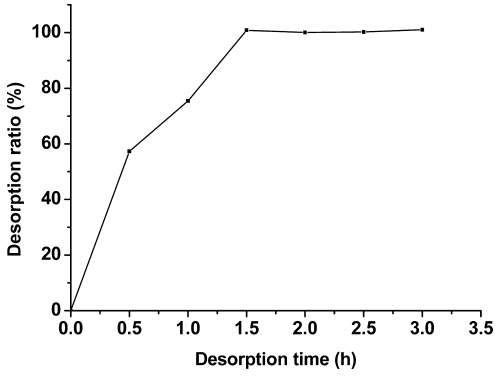

Figure 16. Desorption ratio of sample 6 saturated with Pb^{2+} with the 0.10 mol/L HCl solution.

immigration of Pb^{2+} begins as above-mentioned in the adsorption procedure. The desorption reached the equilibrium within 1.5 h, at which the adsorbed Pb^{2+} was completed eluted from the ATP/FA/PAA beads. This suggests an excellent reusability of ATP/FA/PAA sample 6.

CONCLUSIONS

In this work, two abundant and cheap inorganic materials (micro-scaled FA particles and ATP nanorods) were used as cross-linkers to synthesize the magnetic attapulgite/fly ash/poly(acrylic acid) (ATP/FA/PAA) ternary nanocomposite hydrogels via facile inverse suspension polymerization, instead of the traditional organic cross-linker. The surface modification of the inorganic materials was *in situ* conducted. About 95% of the monomer had been grafted onto the inorganic materials to form the 3-D cross-linking network of the ternary nanocomposite hydrogels in the optimized condition. So, the cost of the ATP/FA/PAA ternary nanocomposite hydrogels is low in view of both raw materials and synthesis. The ternary nanocomposite hydrogels exhibited outstanding mechanical stability due to the large aspect ratio of ATP and showed a certain magnetic characteristic provided by the substantial Fe_3O_4 in FA. The obtained ATP/FA/PAA ternary nanocomposite hydrogels showed a good selective adsorption to Pb^{2+} with a high adsorption capacity of 38 mg/g in 100 mg/L Pb^{2+} solution at pH 5 within 24 h. The adsorbed Pb^{2+} could be totally eluted from the ternary nanocomposite hydrogel adsorbent with 0.10 mol/L HCl aqueous solution within 90 min.

AUTHOR INFORMATION

Corresponding Author

*Tel./Fax: 86 0931 8912582. E-mail: pliu@lzu.edu.cn.

Notes

The authors declare no competing financial interest.

REFERENCES

(1) Wang, X.; Zheng, Y.; Wang, A. Fast removal of copper ions from aqueous solution by chitosan-g-poly(acrylic acid)/attapulgite composites. *J. Hazard. Mater.* **2009**, *168*, 970−977.

(2) Kara, A.; Uzun, L.; Beşirli, N.; Denizli, A. Poly(ethylene glycol dimethacrylate-n-vinyl imidazole) beads for heavy metal removal. *J. Hazard. Mater.* **2004**, *106B*, 93−99.

(3) Wang, H.; Han, Y. J.; Liu, Y.; Bai, T.; Gao, H.; Zhang, P.; Wang, W.; Liu, W. G. High-strength hydrogel as a reusable adsorbent of copper ions. *J. Hazard. Mater.* **2012**, *213*, 258−264.

(4) Ramirez, E.; Burillo, S. G.; Barrera-Diaz, C.; Roa, G.; Bilyeu, B. Use of pH-sensitive polymer hydrogels in lead removal from aqueous solution. *J. Hazard. Mater.* **2011**, *192*, 432−439.

(5) Milosavljevic, N. B.; Ristic, M. D.; Peric-Grujic, A. A.; Fillipovic, J. M.; Strbac, S. B.; Rakocevic, Z. L.; Krusic, M. T. K. Sorption of zinc by novel pH-sensitive hydrogels based on chitosan, itaconic acid and methacrylic acid. *J. Hazard. Mater.* **2011**, *192*, 846−854.

(6) Saber-Samandari, S.; Saber-Samandari, S.; Gazi, M. Cellulose-graft-polyacrylamide/hydroxyapatite composite hydrogel with possible application in removal of Cu (II) ions. *React. Funct. Polym.* **2013**, *73*, 1523−1530.

(7) Natkanski, P.; Kustrowski, P.; Bialas, A.; Piwowarska, Z.; Michalik, M. Thermal stability of montmorillonite polyacrylamide and polyacrylate nanocomposites and adsorption of Fe(III) ions. *Appl. Clay Sci.* **2013**, *75*−*76*, 153−157.

(8) Yu, Z. H.; Zhang, X. D.; Huang, Y. M. Magnetic chitosan-iron(III) hydrogel as a fast and reusable adsorbent for chromium(VI) removal. *Ind. Eng. Chem. Res.* **2013**, *52*, 11956−11966.

(9) Yan, H.; Yang, L. Y.; Yang, Z.; Yang, H.; Li, A. M.; Cheng, R. S. Preparation of chitosan/poly(acrylic acid) magnetic composite microspheres and applications in the removal of copper(II) ions from aqueous solutions. *J. Hazard. Mater.* **2012**, *229*, 371−380.

(10) Liu, P.; Jiang, L. P.; Zhu, L. X.; Wang, A. Q. Attapulgite/poly(acrylic acid) nanocomposite (ATP/PAA) hydrogels with multi-functionalized attapulgite (org-ATP) nanorods as unique cross-linker: Preparation optimization and selective adsorption of Pb(II) ion. *ACS Sustainable Chem. Eng.* **2014**, *2*, 643−651.

(11) Wang, S. B.; Wu, H. W. Environmental-benign utilisation of fly ash as low-cost adsorbents. *J. Hazard. Mater.* **2006**, *136*, 482−501.

(12) Wang, S. Y.; Yang, L.; Zu, Y. G.; Zhao, C. J.; Sun, X. W.; Zhang, L.; Zhang, Z. H. Design and performance evaluation of ionic-liquids-based microwave-assisted environmentally friendly extraction technique for camptothecin and 10-hydroxycamptothecin from Samara of *Camptotheca acuminate*. *Ind. Eng. Chem. Res.* **2011**, *50*, 13620−13627.

(13) Chen, H.; Zhao, J.; Zhong, A. G.; Jin, Y. X. Removal capacity and adsorption mechanism of heat-treated palygorskite clay for Methylene Blue. *Chem. Eng. J.* **2011**, *174*, 143−150.

(14) Yang, C.; Wang, T. M.; Liu, P.; Shi, H. G.; Xue, D. S. Preparation of well-defined blackberry-like polypyrrole/fly ash composite microspheres and their electrical conductivity and magnetic properties. *Curr. Opin. Solid State Mater. Sci.* **2009**, *13*, 112−118.

(15) Mall, I. D.; Srivastava, V. C.; Agarwal, N. K. Removal of Orange G and Methyl Violet dyes by adsorption onto bagasse fly ash—Kinetic study and equilibrium isotherm analyses. *Dyes Pigm.* **2006**, *69*, 210−223.

(16) Jahanzad, F.; Sajjadi, S.; Brooks, B. W. Comparative study of particle size in suspension polymerization and corresponding monomer-water dispersion. *Ind. Eng. Chem. Res.* **2005**, *44*, 4112−4119.

(17) Chatzi, E. G.; Boutris, C. J.; Kiparissides, C. On-line monitoring of drop size distributions in agitated vessels: 2. Effect of stabilizer concentration. *Ind. Eng. Chem. Res.* **1991**, *30*, 1307−1313.

(18) Mendizabal, E.; Castellanos-Ortega, J. R.; Puig, J. E. A method for selecting a poly(vinyl alcohol) as stabilizer in suspension polymerization. *Colloids Surf.* **1992**, *63*, 209−217.

(19) Omidian, H.; Hasherni, S. A.; Askari, F.; Nafisi, S. Swelling and crosslink density measurements for hydrogels. *Polym. Sci. Technol.* **1994**, *3*, 115−119.

(20) Lao, C.; Zelendon, Z.; Gamisans, X.; Sole, M. Sorption of Cd(II) and Pb(II) from aqueous solutions by a low-rank coal (Leonardite). *Sep. Purif. Technol.* **2005**, *45*, 79−85.
(21) Demir-Cakan, R.; Baccile, N.; Antonietti, M.; Titirici, M.-M. Carboxylate-rich carbonaceous materials via one-step hydrothermal carbonization of glucose in the presence of acrylic acid. *Chem. Mater.* **2009**, *21*, 484−490.
(22) Jung, C. H.; Hwang, I. T.; Kuk, I. S.; Choi, J. H.; Oh, B. K.; Lee, Y. M. Poly(acrylic acid)-grafted fluoropolymer films for highly sensitive fluorescent bioassays. *ACS Appl. Mater. Interface* **2013**, *5*, 2155−2160.
(23) Ge, F.; Li, M.; Ye, H.; Zhao, B. Effective removal of heavy metal ions Cd^{2+}, Zn^{2+}, Pb^{2+}, Cu^{2+} from aqueous solution by polymer-modified magnetic nanoparticles. *J. Hazard. Mater.* **2012**, *211−212*, 366−372.
(24) Zheng, Y.; Li, P.; Zhang, J.; Wang, A. Synthesis, characterization and swelling behaviors of poly(sodium acrylate)/vermiculite superabsorbent composites. *Eur. Polym. J.* **2007**, *43*, 1691−1698.
(25) Byun, H.; Hong, B.; Nam, S. Y.; Jung, S. Y.; Rhim, J. W.; Lee, S. B.; Moon, G. Y. Swelling behavior and drug release of poly(vinyl alcohol) hydrogel cross-linked with poly(acrylic acid). *Macromol. Res.* **2008**, *16*, 189−193.
(26) Yeom, Y. H.; Kim, Y. Crystal structure of zeolite X exchanged with Pb(II) at pH 6.0 and dehydrated: $(Pb^{4+})_{14}(Pb^{2+})_{18}(Pb_4O_4)_8Si_{100}Al_{92}O_{384}$. *J. Phys. Chem. B* **1997**, *101*, 5314−5318.
(27) Ozacan, A.; Oncu, E. M.; Ozacan, A. S. Kinetics, isotherm and thermodynamic studies of adsorption of Acid Blue 193 from aqueous solutions onto natural sepiolite. *Colloids Surf, A* **2006**, *277*, 90−97.
(28) Wan Ngah, W. S.; Fatinathan, S. Adsorption characterization of Pb(II) and Cu(II) ions onto chitosan-tripolyphosphate beads: Kinetic, equilibrium and thermodynamic studies. *J. Environ. Manage.* **2010**, *91*, 958−969.
(29) Liang, X.; Su, Y. B.; Yang, Y.; Qin, W. W. Separation and recovery of lead from a low concentration solution of lead(II) and zinc(II) using the hydrolysis production of polystyrene-co-maleic anhydride. *J. Hazard. Mater.* **2012**, *203−204*, 183−187.
(30) Fu, F.; Chen, R.; Xiong, Y. Comparative investigation of N,N′-bis-(dithiocarboxy) piperazine and diethyldithiocarbamate as precipitants for Ni (II) in simulated wastewater. *J. Hazard. Mater.* **2007**, *142*, 437−442.
(31) Moradi, O.; Mirza, B.; Norouzi, M.; Fakhri, A. Removal of Co(II), Cu(II) and Pb(II) ions by polymer based 2-hydroxyethyl methacrylate: Thermodynamics and desorption studies. *J. Environ. Health Sci. Eng.* **2012**, *9*, 31−33.
(32) van Severen, M. C.; Piquemal, J. P.; Parisel, O. Enforcing hemidirectionality in Pb(II) complexes: The importance of anionic ligands. *Chem. Phys. Lett.* **2011**, *510*, 27−30.
(33) Wei, Y. L.; Yang, Y. W.; Lee, J. F. Lead speciation in 0.1N HCl-extracted residue of analog of Pb-contaminated soil. *J. Electron Spectrosc. Relat. Phenom.* **2005**, *144−147*, 299−301.